

# Adaptive Output Feedback for Oil Drilling Stick-Slip Instability Modeled by Wave PDE with Anti-damped Dynamic Boundary

Delphine Bresch-Pietri, Miroslav Krstic

**Abstract**—We develop an adaptive output-feedback controller for a wave PDE in one dimension with actuation on one boundary and with an unknown anti-damping dynamics on the opposite boundary. This model is representative of drill string torsional instabilities arising in deep oil drilling, for which the model of bottom interaction with the rock is poorly known. The key feature of the proposed controller is that it requires only the measurements of boundary values and not of the entire distributed state of the system. Our approach is based on employing Riemann variables to convert the wave PDE into a cascade of two delay elements, with the first of the two delay elements being fed by control and the same element in turn feeding into a scalar ODE. This enables us to employ a prediction-based design for systems with input delays, suitably converted to the adaptive output-feedback setting. The result's relevance and ability to suppress undesirable torsional vibrations of the drill string in oil well drilling systems is illustrated with simulation example.

## I. INTRODUCTION

For oil exploration and production, wells are drilled with a rotating rock-crushing device, called a bit, driven by a rotatory table at the surface, equipped with an electric motor. The torque applied at the surface is transmitted at the bottom of the borehole to the bit through a drill string consisting in various slender tubes. Because of this thinness, the drill string is subject to various vibrations which occur in a strongly nonlinear way due to the interaction with the borehole wall.

In this paper, we consider torsional vibrations leading to the so-called stick-slip phenomenon [7]. Due to its interaction with the rock, the bit slows down and finally stall while the rotatory is still in motion. This causes the bit to be suddenly released after a certain time and to start rotating at very high speed before being slowed down again. Such velocity oscillations give rise to the emission of torsional waves from the lower end, which travel up to the drill string and can reflect from the rotatory table, leading to distributed instabilities. This undesirable limit cycle of the (distributed) drill string velocity can yield to significant malfunctioning or damages of the downhole equipments (bit, drill pipes, electronic devices, etc).

Typically, stick-slip oscillations are combated by developing feedback control in terms of rotatory table motion. Even though researchers have recently investigated the potential of using the so-called weight-on-the-bit at the bottom of the borehole [5] as actuator to act on the strength of the friction

reaction at the bit, such techniques are not commonly used because they have a high risk of collapse due to their bottom location and of subsequent loss of the tool. This is why the application of the torque as ground level is preferred and is the framework under consideration in this paper.

Even if most of the approaches developed in the literature rely on finite dimensional models [8] [15] [20], the drill string torsional dynamics is more accurately represented by a linear wave equation subject to non-linear boundary conditions

representing the top-drive and frictional processes [2] [16]. Lately, by neglecting the effect of damping along the structure, this model has been revisited and the bit dynamics recast as a neutral delay differential equation [19].

In this paper, we follow this overture and develop an adaptive control strategy to handle the high uncertainties on the rock-on-the-bit friction term, which have been proved to be one of the major practical difficulties. Indeed, even if a great number of phenomenological expressions for this nonlinear interaction have been provided over the last decade [13] [15], these models depend on parameters, such as the weigh-on-the-bit or the nature of the rock, that can vary with time and during operation, and are therefore uncertain. To address this point, we consider here two parametric uncertainties appearing linearly in the model.

Following [3] and our recent design [4], we propose, via the introduction of Riemann variables, to reformulate the plant in the form of an input-delay model cascaded with a stable transport equation occurring in the direction opposite from the propagation delay. This formulation allows one to use infinite-dimensional time-delay control strategy, namely, a prediction-based controller, which has recently been reinterpreted in the light of the PDE backstepping technique [10]. Exploiting the transport equation structure of the dynamics under consideration, we present a global output-feedback adaptive controller.

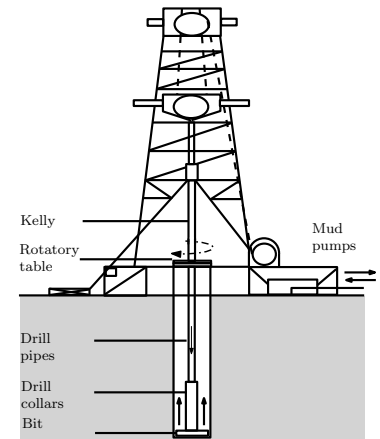


Fig. 1. Schematic view of a drilling system.

D. Bresch-Pietri (corresponding author) is with the Department of Mechanical Engineering, Massachusetts Institute of Technology, Cambridge, MA 02139, USA Email: dbp@mit.edu

M. Krstic is with the Department of Mechanical and Aerospace Engineering, University of California, San Diego, La Jolla CA 92093, USA.

Both the controller and the parameter estimators that we design employ only boundary measurements. This is the main achievement of this paper. While [18] also proposes for the same system an output-feedback control law stabilizing the bit velocity and [11] states an adaptive stabilization result for a similar unstable wave PDE with unmatched parametric uncertainty, the present paper is the first result on *output-feedback adaptive control* providing a  $\mathcal{L}_2$ -norm stabilization result for the entire distributed state.

The paper is organized as follows. In Section II, we describe the system and model challenging, before focusing on Section III on a reformulation of the plant via the introduction of Riemann variables. In Section IV, we present the proposed adaptive controller and the main stabilization result of the paper which is proved in Section V. Finally, Section VI illustrates the relevance and merits of the proposed approach with numerical simulations.

**Notations** In this paper,  $|\cdot|$  is the Euclidean norm and  $\|u(\cdot)\|$  is the spatial  $\mathcal{L}_2$ -norm of a signal  $u(x, \cdot)$ ,  $x \in [0, 1]$ . For  $(a, b) \in \mathbb{R}^2$  such that  $a < b$ , we define the standard projector operator on the interval  $[a, b]$  as a function of two scalar arguments  $f$  (denoting the parameter being update) and  $g$  (denoting the nominal update law) in the following manner:

$$\text{Proj}_{[a,b]}(f, g) = g \begin{cases} 0 & \text{if } f = a \text{ and } g < 0 \\ 0 & \text{if } f = b \text{ and } g > 0 \\ 1 & \text{otherwise} \end{cases}$$

## II. DRILL STRING TORSION MODELING AND CONTROL CHALLENGES

We consider the torsion dynamics of an oil well drill string such as the one pictured in Fig. 1. Following [18], after normalization (see [17]) and neglecting damping, the dynamical equations write

$$u_{tt}(x, t) = u_{xx}(x, t) \quad (1)$$

$$u_x(1, t) = U(t) \quad (2)$$

$$u_{tt}(0, t) = aF(u_t(0, t)) + au_x(0, t) \quad (3)$$

in which  $u$  is the angular displacement of the drill string,  $U$  is the scalar input,

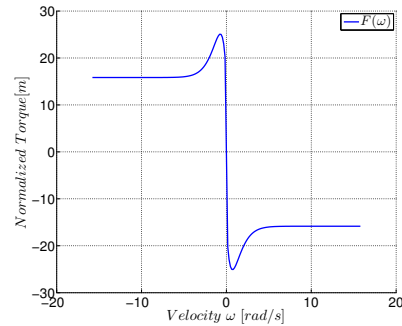


Fig. 2. Rock-on-bit friction term, as a function of the bit angular velocity.

$a > 0$  is constant and  $F$  is a given nonlinear function. In details, the boundary conditions account for two different phenomena: (2) represents the torque actuation of the rotatory table at  $x = 1$  and (3) models the

of the rock, which varies with operation and is also poorly known.

The control objective is to stabilize the angular velocity  $u_t(\cdot, t)$  toward a given uniform rotatory speed  $u_t^r$ . Corresponding steady-state angular displacement profiles are therefore  $u^r(x, t) = u_t^r t - F(u_t^r)x + u_0$  ( $u_0 \in \mathbb{R}$ ) and the corresponding steady-state control law is  $U^r = -F(u_t^r)$ .

Two main difficulties arise while designing control. The first one is visible by considering the error variable  $\tilde{u} = u - u^r$  and the linearized version of (1)–(3) which is

$$\begin{cases} \tilde{u}_{tt}(x, t) &= \tilde{u}_{xx}(x, t) \\ \tilde{u}_x(1, t) &= U(t) - U^r \\ \tilde{u}_{tt}(0, t) &= aq\tilde{u}_t(0, t) + a\tilde{u}_x(0, t) \end{cases} \quad (4)$$

with  $q = \frac{dF}{du_t}(u_t^r)$  unknown. For reasonably large value of  $u_t^r$  (which is the region of interest for drilling operation), one can observe on Fig. 2 that this parameter is positive<sup>1</sup>. The eigenvalues of the uncontrolled system (4) satisfy the equation  $(\sqrt{\lambda} - aq)(1 + e^{2\sqrt{\lambda}}) = a(1 - e^{2\sqrt{\lambda}})$ . Therefore, computing these eigenvalues for a fixed  $q \geq 0$ , one can observe that they are all located in the right-half complex plane. This means that the plant is anti-stable. For small values of  $q$ , some eigenvalues are very close to the origin, generating an oscillatory behavior very similar to the quasi-stable case.

The second difficulty is that, as the function  $F$  is uncertain, not only the boundary condition (2) but also the feedforward term  $U^r$  are poorly known. Therefore, the latter cannot be directly used for control purpose. We address this point by slightly reformulating the plant under consideration in the following section.

## III. PROBLEM STATEMENT AND REFORMULATION

To account for the two difficulties previously discussed, in the following, we investigate closed-loop regulation toward a trajectory  $u^r(x) = dx + u_0$  ( $u_0 \in \mathbb{R}$ ) for the following system<sup>2</sup>

$$u_{tt}(x, t) = u_{xx}(x, t) \quad (5)$$

$$u_x(1, t) = U(t) \quad (6)$$

$$u_{tt}(0, t) = aqu_t(0, t) + a[u_x(0, t) - d] \quad (7)$$

in which  $U(t)$  is the scalar input,  $(u, u_t)$  is the system state, with  $(u(\cdot, 0), u_t(\cdot, 0)) \in H_1([0, 1]) \times L_2([0, 1])$ ,  $a > 0$  is a scalar constant and both the anti-damping parameter  $q > 0$  and the trajectory coefficient  $d \in \mathbb{R}$  are unknown. Besides these uncertainties, the key challenge here is that the source of instability, the “anti-damping” ODE (7), is on the opposite boundary from the boundary that is controlled. Uncertainties are dealt with by employing an adaptive controller, fed by estimates  $\hat{q}(t)$  and  $\hat{d}(t)$  which are updated based on real-time measurements to guarantee closed-loop stability.

<sup>1</sup>Actually, in practice, the torque derivative is positive for any bit velocity. The model employed here does not satisfy this property on a neighborhood of the origin only because, in view of numerical implementation, we consider a smooth approximation of other torque models [9] [15].

<sup>2</sup>In details, this system is the linearized version of (1)–(3) with  $d = -F(u_t^r)$  as unknown parameter and with  $u_t^r = 0$ . This last point is only made for the sake of simplicity of the exposition and can be relaxed straightforwardly (see Section VI).

As always in indirect adaptive control, certain a priori assumptions on the parameter values are needed in order to ensure stabilizability under parameter estimates. For our system, this gives rise to the following assumption.

*Assumption 1:* There exist known constants  $\underline{q}$ ,  $\bar{q}$ ,  $\underline{d}$  and  $\bar{d}$  such that  $\underline{q} < \bar{q}$ ,  $\underline{d} < \bar{d}$  and  $q \in [\underline{q}, \bar{q}]$ ,  $d \in [\underline{d}, \bar{d}]$ .

Besides regulation, a second objective is to design a feedback law which does not employ the distributed state, but only boundary values measurements. We assume that the signals  $u_t(0, \cdot)$  and  $u_t(1, \cdot)$  are measured for all time.

As a first step in our development, we reformulate plant (5)–(7) by introducing the following intermediate Riemann variables and transformed control variable

$$\zeta(x, t) = u_t(x, t) + u_x(x, t) - \hat{d}(t) \quad (8)$$

$$\omega(x, t) = u_t(x, t) - u_x(x, t) + \hat{d}(t) \quad (9)$$

$$W(t) = u_t(1, t) + U(t) - \hat{d}(t) \quad (10)$$

which lead to the following new dynamics, with the estimation error  $\tilde{d}(t) = d - \hat{d}(t)$ ,

$$u_{tt}(0, t) = a(q-1)u_t(0, t) + a[\zeta(0, t) - \tilde{d}(t)] \quad (11)$$

$$\zeta_t(x, t) = \zeta_x(x, t) - \hat{d}(t) \quad (12)$$

$$\zeta(1, t) = W(t) \quad (13)$$

$$\omega_t(x, t) = -\omega_x(x, t) + \hat{d}(t) \quad (14)$$

$$\omega(0, t) = 2u_t(0, t) - \zeta(0, t) \quad (15)$$

In this new framework, the wave phenomenon is represented as the cascade of two transport PDEs with source term, with one ODE being driven by the first of the two PDEs. The ODE (11) with state  $u_t(0, \cdot)$  plays a central role and it has to be made asymptotically stable by feedback, which is applied through the transport equation (12) controlled at the boundary  $x = 1$ . A second transport phenomenon (14) with similar source term is also present, in the opposite direction, accounting for the reflection of the wave at  $x = 0$ .

*Remark 1:* From the transport equations (12) and (14), we have that  $\zeta(x, t) = \zeta(y, t+x-y) - \hat{d}(t) + \hat{d}(t+x-y)$  and  $\omega(x, t) = \omega(y, t-x+y) + \hat{d}(t) - \hat{d}(t-x+y)$  for any  $0 \leq y \leq x \leq 1$  and any  $t \geq 0$ .

In particular,  $\zeta(x, t) = W(t-1+x) - \hat{d}(t) + \hat{d}(t-1+x)$ ,  $x \in [0, 1]$  and  $t \geq 0$ , and  $\omega(x, t) = \omega(0, t-x) + \hat{d}(t) - \hat{d}(t-x) = 2u_t(0, t-x) - W(t-1-x) + \hat{d}(t) - \hat{d}(t-1-x)$ .

Following [10], when  $\hat{d}(t) = 0$ , (11)–(13) can also be interpreted as an input-delay ordinary differential equation, delayed by 1 unit of time, followed by a stable transport phenomenon (14)–(15). This motivates the control design.

#### IV. CONTROL DESIGN

Consider the following control law

$$U(t) = -u_t(1, t) + \hat{d}(t) - (c_0 + \hat{q}(t) - 1) \left( e^{a(\hat{q}(t)-1)} u_t(0, t) + a \int_{t-1}^t e^{a(\hat{q}(t)-1)(t-\tau)} [\eta(\tau) - \hat{d}(t)] d\tau \right) \quad (16)$$

in which  $c_0 > 0$  is a constant,  $\hat{q}$  is an estimate of the unknown parameter  $q$  and  $\eta(t) = U(t) + u_t(1, t)$ . We design the parameter estimate update laws as

$$\dot{\hat{q}}(t) = \frac{a\gamma_q}{1+N(t)} \text{Proj}_{[\underline{q}, \bar{q}]} \left\{ \hat{q}(t), u_t(0, t) \left( u_t(0, t) + b_1(c_0 + \hat{q}(t) - 1) \int_{t-1}^t e^{(a(\hat{q}(t)-1)+1)(\tau-t+1)} w(\tau, t) d\tau \right) \right\} \quad (17)$$

$$\dot{\hat{d}}(t) = \frac{a\gamma_d}{1+N(t)} \text{Proj}_{[\underline{d}, \bar{d}]} \left\{ \hat{d}(t), -u_t(0, t) - b_1(c_0 + \hat{q}(t) - 1) \int_{t-1}^t e^{(a(\hat{q}(t)-1)+1)(\tau-t+1)} w(\tau, t) d\tau \right\} \quad (18)$$

$$N(t) = u_t(0, t)^2 + b_1 \int_{t-1}^t e^{\tau-t+1} w(\tau, t)^2 d\tau + b_2 \int_{t-1}^t e^{t-\tau} (2u_t(0, \tau) - \eta(\tau-1) + \hat{d}(t))^2 d\tau \quad (19)$$

in which the bounds  $\underline{q}, \bar{q}, \underline{d}, \bar{d}$  are defined in Assumption 1, Proj is the standard projection operator, the normalization constants  $b_1, b_2 > 0$  and the update gains  $\gamma_d, \gamma_q > 0$  are tuning parameters and, for  $t \geq 0$  and  $t-1 \leq \tau \leq t$ ,

$$w(\tau, t) = \eta(\tau) - \hat{d}(t) + (c_0 + \hat{q}(t) - 1) \left( e^{a(\hat{q}(t)-1)(\tau-t+1)} u_t(0, t) + a \int_{t-1}^{\tau} e^{a(\hat{q}(t)-1)(\tau-\xi)} [\eta(\xi) - \hat{d}(t)] d\xi \right) \quad (20)$$

In order to properly interpret this adaptive control law, we provide several comments next.

The choice of the control law (16) originates from the interpretation of (11)–(13) as an input delay system. Indeed, if  $q$  and  $d$  were known, one could simply choose  $\hat{d} = d$  and define  $\zeta(x, t) = \eta(t+x-1) - d$ , following Remark 1. Then, the following predictor-based control law [1] [14] would compensate exactly the delay

$$W(t) = -(c_0 + q - 1) \left( e^{a(q-1)} u_t(0, t) + a \int_0^1 e^{a(q-1)(1-x)} [\eta(t+x-1) - d] dx \right) \quad (21)$$

i.e., after 1 unit of time, it would result into the closed-loop dynamics  $u_{tt}(0, t) = -c_0 u_t(0, t)$  which is exponentially stable for any  $c_0 > 0$ . Then, with a suitable change of variable and applying the certainty equivalence principle, the control law (16) follows.

The choice of the update laws is based on Lyapunov design, as detailed in the following section. As common in adaptive control [6] [12], a projector operator is used in (17)–(18). In addition, normalization (19) is employed in order to limit the rate of change of the parameter estimate, which could otherwise act as a destabilizing disturbance.

As a final remark, we would like to stress the fact that the proposed controller (16)–(20) is entirely computable with only the measurement of the boundary values  $u_t(0, \cdot)$  and  $u_t(1, \cdot)$ . This is the main advantage of this control law compared to ones previously obtained, like e.g. in [17] which requires the measurement of the entire distributed state.

*Theorem 1:* Consider the closed-loop system consisting of the plant (5)-(7), the control law (16) and the parameter update laws (17)-(20). Define the functional

$$\begin{aligned} \Gamma(t) = & u_t(0,t)^2 + \int_0^1 u_t(x,t)^2 dx + \int_0^1 (u_x(x,t) - d)^2 dx \\ & + (q - \hat{q}(t))^2 + (d - \hat{d}(t))^2 \end{aligned} \quad (22)$$

For any  $c_0 > 0$ , there exists positive constants  $b_2^*(c_0)$ ,  $b_1^*(c_0, b_2^*)$ ,  $\gamma^*(c_0, b_1^*, b_2^*)$  such that, provided that  $b_2 < b_2^*$ ,  $b_1 > b_1^*$ ,  $\gamma_d \in (0, \gamma^*)$  and  $\gamma_q \in (0, \gamma^*)$ , then there exist  $R > 0$  and  $\rho > 0$  such that

$$\Gamma(t) \leq R(e^{\rho\Gamma(0)} - 1) \quad (23)$$

and the regulation in  $\mathcal{L}_2$ -norm follows, i.e.

$$\begin{aligned} \lim_{t \rightarrow \infty} u_t(0,t) = & \lim_{t \rightarrow \infty} \|u_t(t)\| \\ = & \lim_{t \rightarrow \infty} \|u_x(t) - d\| = \lim_{t \rightarrow \infty} (\hat{d}(t) - d) = 0 \end{aligned} \quad (24)$$

We now provide the proof of this theorem, before applying it to the drill string torsion dynamics and illustrating its merits with simulations.

## V. PROOF OF THEOREM 1

### A. Backstepping transformation and target system

Consider the backstepping transformation of the distributed variable  $\zeta$

$$\begin{aligned} z(x,t) = & \zeta(x,t) + (c_0 + \hat{q}(t) - 1) \left( e^{a(\hat{q}(t)-1)x} u_t(0,t) \right. \\ & \left. + a \int_0^x e^{a(\hat{q}(t)-1)(x-y)} \zeta(y,t) dy \right) \end{aligned} \quad (25)$$

Following Remark 1 and with a suitable change of variable, one can observe that this transformation is closely related to (20) with  $z(x,t) = w(t-1+x,t)$ ,  $x \in [0, 1]$ ,  $t \geq 0$ . Using this relation and some changes of variable, the control law (16) can be rewritten in terms of the distributed variable  $\zeta$  as

$$\begin{aligned} W(t) = & -(c_0 + \hat{q}(t) - 1) \left( e^{a(\hat{q}(t)-1)} u_t(0,t) \right. \\ & \left. + a \int_0^1 e^{a(\hat{q}(t)-1)(1-x)} \zeta(x,t) dx \right) \end{aligned} \quad (26)$$

The plant (11)–(15) can then be reformulated as the following target system

$$u_{tt}(0,t) = -c_0 a u_t(0,t) + a[z(0,t) + \tilde{q}(t)u_t(0,t) - \tilde{d}(t)] \quad (27)$$

$$z_t = z_x + \hat{q}g_q(x,t) + \hat{d}g_d(x,t) + [\tilde{q}(t)u_t(0,t) - \tilde{d}(t)]h(x,t) \quad (28)$$

$$z(1,t) = 0 \quad (29)$$

$$\omega_t = -\omega_x + \hat{d}(t) \quad (30)$$

$$\omega(0,t) = (c_0 + \hat{q} + 1)u_t(0,t) - z(0,t) \quad (31)$$

in which  $\tilde{q}(t) = q - \hat{q}(t)$  is the anti-damping parameter estimation error and

$$g_q(x,t) = e^{a(\hat{q}(t)-1)x} u_t(0,t) + a \int_0^x e^{a(\hat{q}(t)-1)(x-y)} \zeta(y,t) dy$$

$$\begin{aligned} & + (c_0 + \hat{q}(t) - 1) \left( a x e^{a(\hat{q}(t)-1)x} u_t(0,t) \right. \\ & \left. + a^2 \int_0^x (x-y) e^{a(\hat{q}(t)-1)(x-y)} \zeta(y,t) dy \right) \end{aligned} \quad (32)$$

$$g_d(x,t) = -1 - (c_0 + \hat{q}(t) - 1) a \int_0^x e^{a(\hat{q}(t)-1)(x-y)} dy \quad (33)$$

$$h(x,t) = a(c_0 + \hat{q}(t) - 1) e^{a(\hat{q}(t)-1)x} \quad (34)$$

This target system is the one which is exploited in the Lyapunov analysis, as it presents the advantage of having a boundary condition  $z(1,t) = 0$ .

### B. Lyapunov analysis

We are now ready to start the Lyapunov analysis. Define the Lyapunov-Krasovskii functional candidate

$$V(t) = \log(1 + N(t)) + \frac{\tilde{q}(t)^2}{\gamma_q} + \frac{\tilde{d}(t)^2}{\gamma_d} \quad (35)$$

in which, following Remark 1, the normalization factor originally defined in (19) can be expressed as

$$N(t) = u_t(0,t)^2 + b_1 \int_0^1 e^x z(x,t)^2 dx + b_2 \int_0^1 e^{1-x} \omega(x,t)^2 dx \quad (36)$$

Note that similarly, the update laws (17)–(18) can be reformulated in terms of the backstepping transformation  $z(x, \cdot)$ . Taking a time-derivative of (35), using projection operator properties and (17)–(19), one obtains

$$\begin{aligned} \dot{V}(t) \leq & \frac{1}{1+N(t)} \left( -2c_0 a u_t(0,t)^2 - b_1 z(0,t)^2 - b_1 \|z(t)\|^2 \right. \\ & + 2a u_t(0,t) z(0,t) + 2b_1 \hat{q}(t) \int_0^1 e^x z(x,t) g_q(x,t) dx \\ & + 2b_1 \hat{d}(t) \int_0^1 e^x z(x,t) g_d(x,t) dx + b_2 \left( e\omega(0,t)^2 \right. \\ & \left. - \|\omega(t)\|^2 + 2\hat{d}(t) \int_0^1 e^{1-x} \omega(x,t) dx \right) \end{aligned} \quad (37)$$

Applying Young and Cauchy-Schwartz inequalities, one gets the existence of  $M_1(b_1), M_2(b_1) > 0$  and  $M_3 > 0$  such that

$$\left| 2\hat{q}(t) \int_0^1 e^x z(x,t) g_q(x,t) dx \right| \leq \gamma_q M_1(b_1) (u_t(0,t)^2 + \|z(t)\|^2) \quad (38)$$

$$|\hat{d}(t)| \leq \gamma_d M_2(b_1) \quad (39)$$

$$\left| 2 \int_0^1 e^x z(x,t) g_d(x,t) dx \right| \leq M_3 (u_t(0,t)^2 + \|z(t)\|^2) \quad (40)$$

Similarly, applying again Young inequality and using that  $1 + N(t) \geq 1$ , one can obtain the existence of  $M_4 > 0$  such that

$$\left| \frac{2\hat{d}(t)}{\gamma_d} \int_0^1 e^{1-x} \omega(x,t) dx \right| \leq M_4 (u_t(0,t)^2 + \|z(t)\|^2 + \|\omega(t)\|^2) \quad (41)$$

Consequently, using (31) and Young inequality, it follows

$$\dot{V}(t) \leq \frac{1}{1+N(t)} \left( - \left( b_1 - \frac{a}{c_0} - 2eb_2 \right) z(0,t)^2 - \left( \frac{ac_0}{2} \right. \right.$$

$$\begin{aligned}
& -\gamma_q M_1(b_1) - 2eb_2(1+c_0+\hat{q})^2 - \gamma_d M_2(b_1) M_3 \\
& - \gamma_d b_2 M_4) u_t(0,t)^2 - b_2(1-\gamma_d b_2 M_4) \|\omega(t)\|^2 \\
& - (b_1 - \gamma_q M_1(b_1) - \gamma_d M_3 M_2(b_1) - \gamma_d b_2 M_4) \|z(t)\|^2) \quad (42)
\end{aligned}$$

Therefore, by choosing  $b_2 < \frac{ac_0}{4e(1+c_0+\bar{q})^2}$ ,  $b_1 > \frac{a}{c_0} + 2eb_2$  and  $\gamma_q + \gamma_d < \frac{\min\{ac_0 - 4eb_2(1+c_0+\bar{q})^2, 2b_1, 2\}}{2\max\{M_1(b_1), M_3 M_2(b_1), b_2 M_4\}}$ , there exists  $\eta > 0$  such that

$$\dot{V}(t) \leq -\frac{\eta}{N(t)} \left( u_t(0,t)^2 + \|z(t)\|^2 + \|\omega(t)\|^2 \right) \quad (43)$$

and finally

$$V(t) \leq V(0), t \geq 0 \quad (44)$$

### C. Stability in terms of the functional $\Gamma$

Finally, we need to establish the stability in terms of  $\Gamma$ . First, from the Riemann variables definition (8)-(9), one gets

$$u_t(x,t) = \frac{\zeta(x,t) + \omega(x,t)}{2} \quad (45)$$

$$u_x(x,t) - \hat{d}(t) = \frac{\zeta(x,t) - \omega(x,t)}{2} \quad (46)$$

Second, from (25) and its inverse

$$\begin{aligned}
\zeta(x,t) = & z(x,t) - (c_0 + \hat{q} - 1) \left( e^{-ac_0 x} u_t(0,t) \right. \\
& \left. + a \int_0^x e^{-ac_0(x-y)} z(y,t) dy \right) \quad (47)
\end{aligned}$$

applying Young and Cauchy-Schwartz inequalities, one shows that there exist  $r_1, r_2, s_1, s_2 > 0$  such that

$$\|\zeta(t)\|^2 \leq r_1 u_t(0,t)^2 + r_2 \|z(t)\|^2 \quad (48)$$

$$\|z(t)\|^2 \leq s_1 u_t(0,t)^2 + s_2 \|\zeta(t)\|^2 \quad (49)$$

Consequently, with these inequalities and Young inequality, it follows that

$$\Gamma(t) \leq \left( 1 + \frac{3}{2} \left( r_1 + \frac{r_2}{b_1} + \frac{1}{b_2} \right) + \gamma_q + 3\gamma_d \right) (e^{V(t)} - 1) \quad (50)$$

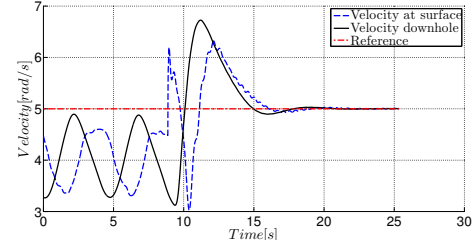
$$V(t) \leq \left( 1 + b_1 e^{(s_1 + 2s_2)} + 2eb_2 + \frac{1}{\gamma_q} + \frac{1}{\gamma_d} \right) \Gamma(t) \quad (51)$$

Matching the two previous inequalities with (44) gives the stability result stated in the Theorem.

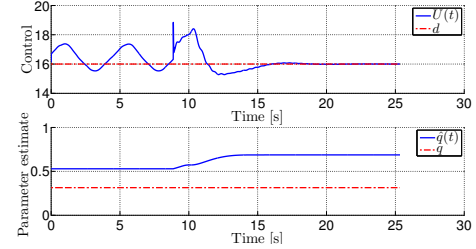
### D. Convergence analysis

From (44), one can easily get that  $N(t)$ ,  $\tilde{q}$  and  $\tilde{d}$  are uniformly bounded for  $t \geq 0$ , and therefore  $u_t(0,t)$ ,  $\|z(t)\|$  and  $\|\omega(t)\|$  are also uniformly bounded for  $t \geq 0$ . Consequently, from (48),  $\|\zeta(t)\|$  is also uniformly bounded for  $t \geq 0$ .

From there, applying Young inequality to (17), one can obtain that  $\hat{q}$  is uniformly bounded for  $t \geq 0$ . Similarly, applying Cauchy-Schwartz inequality to (16), one can obtain that  $\zeta(1,t)$  is uniformly bounded for  $t \geq 0$ . Further, as  $\zeta(x,t) = \zeta(1,t-1+x) - \hat{d}(t) + \hat{d}(t-1+x)$ ,  $\zeta(x,t)$  is also



(a) Velocity evolution. The adaptive controller is turned on after 9 sec.



(b) Control input and parameter estimate evolutions. The adaptive controller is turned on after 9 sec.

Fig. 3. Stabilization of plant (1)–(3) using the output-feedback adaptive controller proposed in Theorem 1 for the unknown parameters  $d = -F(u_t^r)$  and  $q = \frac{dF}{du_t}(u_t^r)$  ( $c_0 = 1/a$ ,  $\gamma_d = 1$ ,  $\gamma_q = 0.1$  and  $b_1 = 1e-3$ ,  $b_2 = 0.1$ ).

uniformly bounded for  $t \geq 1-x$  and in particular  $\zeta(0,t)$  is uniformly bounded for  $t \geq 1$ . From (25),

$$z(0,t) = \zeta(0,t) + (c_0 + \hat{q} - 1)u_t(0,t) \quad (52)$$

and, consequently,  $z(0,t)$  is also uniformly bounded for  $t \geq 1$ . Further, from (27)-(31), applying integrations by parts, one can express  $du_t(0,t)^2/dt$ ,  $d\|z(t)\|^2/dt$  and  $d\|\omega(t)\|^2/dt$  and, using (32)–(34), (17)–(18), Cauchy-Schwartz inequality and the previous considerations, obtain their uniform boundedness for  $t \geq 2$ .

Finally, integrating (43) from 0 to  $\infty$ , it follows that  $u_t(0,t)$ ,  $\|z(t)\|$  and  $\|\omega(t)\|$  are square integrable. Following Barbalat Lemma,  $u_t(0,t)$ ,  $\|z(t)\|$  and  $\|\omega(t)\|$  tend to zero as  $t$  tends to  $\infty$ . Using (45)-(46), it follows that  $\|u_t(t)\|$  and  $\|u_x(t) - \hat{d}(t)\|$  tend to zero as  $t$  tends to  $\infty$ . The result follows from there using (7) and (18).

## VI. NUMERICAL SIMULATIONS

In this section, we present numerical simulations illustrating the behavior and merits of the proposed adaptive controller (16)–(19). To give physical insight on its performances, simulations results are provided in physical coordinate, i.e. using the model proposed in [18] which is equivalent to (1)–(3) (see [17]). The model parameters used in simulations are taken from [17] to ease performance comparisons and gathered in Table I.

The adaptive-controller (16)–(20) is used for regulation instead of stabilization by simply using  $u_t(0,\cdot) - u_t^r$  in the controller equations in lieu of  $u_t(0,\cdot)$ . Velocity reference is chosen as  $\theta_t^r = 5$  rad/s (or equivalently  $u_t^r \approx 3$  s<sup>-1</sup>). Corresponding unknown parameter are therefore  $d = -F(u_t^r) = 16$  and  $q = \frac{\partial F}{\partial u_t}(u_t^r) = 0.31$ . Initial parameters estimates are obtained with an incorrect rock-on-bit friction function and are  $\hat{d}(0) = 16.15$  and  $\hat{q}(0) = 0.53$ . The control gain is chosen such that  $c_0 a = 1$ .

The controller is turned on after 9 s. One can observe that the open-loop system not only exhibits a oscillatory behavior, as previously discussed, but is also biased because of the uncertainty of the rock-on-bit friction term which is used as feedforward. The proposed closed-loop strategy efficiently suppresses both of these effects. Specifically, the essence of the controller behavior is particularly visible on Fig. 3(a): the control computed at  $t = 9$  sec starts acting on the bit velocity at  $t \approx 10$  s, which is consistent with the physical system propagation time  $T = .6$  (see [17] and Table I) and the bit velocity then converges in an exponential manner to its reference, as could be expected from the control choice. The velocity of the rotatory table follows a similar trend delayed by  $T \approx .6$  s which corresponds to the time needed for the control law to propagate back to the surface. Fig. 3(b) pictures the variation of the parameter estimates. As stated in Theorem 1, the rock-on-bit friction term  $d$  is asymptotically estimated. On the other hand, the estimate of the anti-damping coefficient does converge but not to the unknown parameter, even if stabilization is achieved. This behavior well-known in adaptive control [6] is consistent with the error equations.

The obtained performance compares favorably to ones previously obtained in the literature [17], [20]. An interesting property of our controller is that, by compensating the propagation delay, transient behavior is particularly smooth, compared to the damping obtained in [20] for example, and, besides, tunable via the feedback gain  $c_0$ . On the other hand, its settling time cannot be arbitrarily decreased as the input delay is only suffered here, meaning that we have chosen to act on the dynamics (11)–(13) and to let the asymptotic regulation of the second transport PDE (14)–(15) stemming from the one of the first ODE-PDE cascade. This choice leads to a settling time greater or equal to twice the propagation delay, and therefore superior to the one obtained in [17] for example, where the second dynamics is actively stabilized. However, contrary to the one presented here, the distributed controller proposed in [17] requires the knowledge of the distributed state.

## VII. CONCLUSION

In this paper, we have proposed an adaptive output-feedback control law for a wave PDE with unknown anti-damping dynamic boundary and showed the interest of the proposed technique to suppress undesirable torsional vibrations of a drilling system. The main advantage of our controller is that it does not require the knowledge of the entire system state but only on the top and bottom velocities. However, in practice, the latter is not only extremely noisy but also substantially delayed, as the signal is either transmitted via the mud system flowing back to the surface or via dedicated acoustic waves, both solutions generating a (time-varying) transport delay [8]. Design of a bottom velocity observer to address this point is a direction of future work.

## REFERENCES

[1] Z. Artstein. Linear systems with delayed controls: a reduction. *IEEE Transactions on Automatic Control*, 27(4):869–879, 1982.

Symbol	Description	Value
$G$	Shear modulus of the drill pipe	$79.6 \text{ e}10 \text{ N/m}^2$
$I$	Drill pipe moment of inertia per unit of length	0.095 kg.m
$I_B$	Moment of inertia of the BHA	311 kg.m <sup>2</sup>
$J$	Drill pipe second moment of area	$1.19 \text{ e-}5 \text{ m}^4$
$L$	Length of the drill pipe	2000 m
$T_{rob}$	Torque on the bit parameter	7500 N.m
$\alpha_1, \alpha_2, \alpha_3$	Friction parameters	5.5; 2.2;3500
$\gamma$	Damping parameter	0.03 N.m.s /rad

BHA stands for Bottom Hole Assembly (bit and drill collars, see Fig. 1).

TABLE I

LIST OF THE PARAMETERS USED IN SIMULATIONS (SEE [17] FOR PHYSICAL MODELING AND NORMALIZATION).

- [2] A. G. Balanov, N. B. Janson, P. V. Mc Clintock, R. W. Tucker, and C. H. T. Wang. Bifurcation analysis of a neutral delay differential equation modelling the torsional motion of a driven drill-string. *Chaos, Solitons & Fractals*, 15(2):381–394, 2003.
- [3] N. Bekiaris-Liberis and M. Krstic. Compensation of wave actuator dynamics for nonlinear systems. *IEEE Transactions on Automatic Control*, to appear.
- [4] D. Bresch-Pietri and M. Krstic. Output-feedback adaptive control of a wave PDE with boundary anti-damping. *Automatica*, to appear.
- [5] C. Canudas-de Wit, F. R. Rubio, and M. A. Corchero. D-oski: A new mechanism for controlling stick-slip oscillations in oil well drillstrings. *IEEE Transactions on Control Systems Technology*, 16(6):1177–1191, 2008.
- [6] P. A. Ioannou and B. Fidan. *Adaptive Control Tutorial*. Society for Industrial Mathematics, 2006.
- [7] J. D. Jansen and L. Van den Steen. Active damping of self-excited torsional vibrations in oil well drillstrings. *Journal of Sound and Vibration*, 179(4):647–668, 1995.
- [8] R. B. Jijón, C. Canudas-de Wit, S. Niculescu, and J. Dumon. Adaptive observer design under low data rate transmission with applications to oil well drill-string. In *American Control Conference*, 2010.
- [9] D. Karnopp. Computer simulation of stick-slip friction in mechanical dynamic systems. *ASME Journal of Dynamics Systems, Measurement and Control*, 107:100–103, 1985.
- [10] M. Krstic. *Boundary Control of PDEs: a Course on Backstepping Designs*. Society for Industrial and Applied Mathematics Philadelphia, PA, USA, 2008.
- [11] M. Krstic. Adaptive control of an anti-stable wave PDE. *Dynamics of Continuous, Discrete and Impulsive Systems*, 17:853–882, 2010.
- [12] M. Krstic, I. Kanellakopoulos, and P.V. Kokotovic. *Nonlinear and Adaptive Control Design*. John Wiley & Sons New York, 1995.
- [13] L. Li, Q. Zhang, and N. Rasol. Time-varying sliding mode adaptive control for rotary drilling system. *Journal of Computers*, 6(3):564–570, 2011.
- [14] A. Manitius and A. Olbrot. Finite spectrum assignment problem for systems with delays. *IEEE Transactions on Automatic Control*, 24(4):541–552, 1979.
- [15] E. M Navarro-López and D. Cortés. Sliding-mode control of a multi-dof oilwell drillstring with stick-slip oscillations. In *American Control Conference*, 2007.
- [16] P. Rouchon. Flatness and stick-slip stabilization. Technical report, MINES ParisTech, 1998.
- [17] C. Sagert, F. Di Meglio, M. Krstic, and P. Rouchon. Backstepping and flatness approaches for stabilization of the stick-slip phenomenon for drilling. In *IFAC Symposium on System, Structure and Control*, 2013.
- [18] M. B. Saldivar, S. Mondié, J.-J. Loiseau, and V. Rasvan. Stick-slip oscillations in oilwell drillstrings: distributed parameter and neutral type retarded model approaches. In *IFAC 18th World Congress*, pages 283–289, 2011.
- [19] M. B. Saldivar, A. Seuret, and S. Mondié. Exponential stabilization of a class of nonlinear neutral type time-delay systems, an oilwell drilling model example. In *International Conference on Electrical Engineering Computing Science and Automatic Control*, pages 1–6. IEEE, 2011.
- [20] A. Serrarens, M. Van de Molengraft, J. Kok, and L. Van den Steen.  $H_\infty$  control for suppressing stick-slip in oil well drillstrings. *Control Systems, IEEE*, 18(2):19–30, 1998.